Modulation of tropical cyclones in the southeastern part of western North Pacific by tropical Pacific decadal variability

Chao Liu[1] · Wenjun Zhang[1] · Xin Geng[1] · Malte F. Stuecker[2,3] · Fei-Fei Jin[4]

Abstract

The tropical cyclone (TC) genesis number in the western North Pacific (WNP) exhibits a pronounced decadal decrease around the mid-1990s, with prominent seasonal and spatial inhomogeneity. This decadal shift of TC activity is mostly confined to the southeastern part of the WNP and occurs mainly during the second half of the calendar year. Accordingly, westward and northeastward TC recurving movements strongly decreased in recent decades after 1995 compared with TC tracks in the earlier period (1979–1994). We find that this TC activity decadal change is associated with tropical Pacific decadal variability, which is measured here by a low-pass filtered Niño3.4 index. In contrast to the earlier period, the anomalous cold mean state in the tropical Pacific during recent decades favored the enhancement of zonal vertical wind shear (UVWS) and suppressed TC activity. This tropical Pacific mean state change is possibly related to decadal changes of El Niño–Southern Oscillation (ENSO) properties (i.e., more La Niña events occurred during recent decades). This relationship between tropical Pacific mean state change and the UVWS in the southeastern WNP on decadal timescales is further validated based on longer observations (1951–2017) and control simulations from the Coupled Model Intercomparison Project Phase 5 (CMIP5). The statistical relationships between TC activity and the Pacific Decadal Oscillation (PDO) or Atlantic Multidecadal Oscillation (AMO) are weaker and insignificant, both for the observations and for simulations. Our results imply that decadal variations of the tropical Pacific mean state should be taken into account when predicting WNP TC activities on decadal timescales.

Keywords Tropical cyclone · Decadal change · Tropical Pacific decadal variability

1 Introduction

As one of the most active regions for tropical cyclones (TCs) in the world, the western North Pacific (WNP) basin witnesses about 26 TCs each year, which cause severe flooding and massive socioeconomic losses in coastal Asian countries (Peduzzi et al. 2012). Considering its disastrous impacts, TC activity has received widespread concerns for local policy makers and within the scientific community (Zhan et al. 2012; Zhang et al. 2017a). Numerous efforts have been made in recent decades to improve our understanding of the temporal and spatial variability of WNP TC activity (e.g., Wang and Chan 2002; Chen and Tam 2010; Knutson et al. 2010; Kim et al. 2011; Liu and Chan 2013; Zhao et al. 2018a).

WNP TCs exhibit pronounced variability on multiple timescales due to various climate forcings (e.g., Wang and Chan 2002; Vecchi and Soden 2007; Kim et al. 2008; Zhan et al. 2013; Li and Zhou 2013; Wang et al. 2015; Lin and Chan 2015; Mei and Xie 2016). For instance, it has been shown that on intraseasonal timescales (30- to 90-days), the Madden–Julian Oscillation (MJO) modulates WNP TC activity (e.g., Li and Zhou 2013; Wang et al. 2018b; Zhao et al. 2019). During the active-phase of the MJO in the WNP, local convection is enhanced, which in turn leads to increased TC activity in the basin. Another intraseasonal mode known as quasi-biweekly oscillation (QBWO) also affects the WNP TC activity, but with a more localized effect (Li and Zhou 2013).

✉ Wenjun Zhang
  zhangwj@nuist.edu.cn

[1] CIC-FEMD/ILCEC, Key Laboratory of Meteorological Disaster of Ministry of Education, School of Atmospheric Sciences, Nanjing University of Information Science and Technology, Nanjing 210044, China

[2] Center for Climate Physics, Institute for Basic Science (IBS), Busan, Republic of Korea

[3] Pusan National University, Busan, Republic of Korea

[4] Department of Atmospheric Sciences, SOEST, University of Hawai'i at Manoa, Honolulu, USA

On interannual timescales, variability of WNP TC activity is argued to be associated with different large-scale climate processes, such as the tropical Pacific sea surface temperature (SST) state (Wang and Chan 2002; Camargo and Sobel 2005; Zhan et al. 2013; Zhang et al. 2016), northern Indian Ocean SST anomalies (Zhan et al. 2011; Tao et al. 2012), and Atlantic SST anomalies (Huo et al. 2015; Zhang et al. 2017b). Among them, El Niño-Southern Oscillation (ENSO), the predominant source of global interannual climate variability (e.g., Wallace et al. 1998; Trenberth and Caron 2000; Timmermann et al. 2018), has been extensively reported to have important impacts on WNP TC activity (e.g., Wang and Chan 2002; Camargo and Sobel 2005; Kim et al. 2011). During summer of the developing year for the warm ENSO phase (i.e., El Niño), WNP TCs tend to form close to the equator and dateline with preferred northeastward recurved tracks. It usually takes a relatively long time for these TCs to make landfall or to decay into extratropical cyclones, which leads to an increased TC intensity because they tend to derive more energy from the warm ocean (Camargo and Sobel 2005). In contrast, TC activity is generally reduced in the WNP during the El Niño decaying phase, due to the strong anticyclonic circulation anomalies and increased subsidence in the WNP (e.g., Wang and Chan 2002; Du et al. 2011). The response of TC activity to the ENSO cold phase (i.e., La Niña) exhibits roughly the opposite pattern. Compared to the traditional El Niño (SST anomaly center is located in eastern Pacific), another type of El Niño was frequently observed in recent decades, whose air-sea action center is shifted to the central Pacific (CP El Niño) (e.g., Ashok et al. 2007; Kao and Yu 2009; Kug et al. 2009). As a consequence of the westward shifted SST anomaly center and corresponding convective heating shift, CP El Niño events are usually accompanied by a basin-wide enhancement of TC activity during boreal summer (Chen and Tam 2010; Kim et al. 2011; Wang et al. 2013). Unlike the traditional El Niño, CP El Niño typically exhibits only a minor suppression effect on TC activity during its decaying phase, due to the weaker WNP anticyclonic circulation anomalies associated with it (Zhang et al. 2015; Wang et al. 2018a). Apart from genesis number and location, the number of landfall events also tend to be different. In the summer of CP El Niño developing years, TCs are generally more likely to make landfall over East Asia compared to the year of traditional El Niño (Zhang et al. 2012). Thus, the existence of different ENSO flavors results in a more complicated ENSO-TC relationship.

Due to the shortness of TC records and temporal inhomogeneity of datasets, TC variability on decadal timescales is not well understood yet. Earlier studies argued that variability of TC activity over the WNP is characterized by periodicities of about 16–32 years, which may be related to the combined effects of monsoon trough position and strength variability, as well as central Pacific SST anomalies or modulation effects of the Pacific Decadal Oscillation (PDO) (Matsuura et al. 2003; Chan 2008; Camargo et al. 2010). Most recent observations seem to suggest that WNP basin-wide TC activity underwent a decadal change around the mid-to-late 1990s. Since then, both the genesis number and duration of TCs decreased rather abruptly, which was also accompanied by more preferred northwestward tracks. Besides, TC activity in the South China Sea (SCS) also increased after the 1994. More TCs recurve to the northeast and eventually enter into the East China Sea and Philippine Sea since this time. This active period, however, ceased at the begin of the twenty-first century (Ha et al. 2014; Li and Zhou 2014; Ha and Zhong 2015).

Many potential factors have been proposed to explain this basin-wide decadal shift, such as a strengthened western North Pacific subtropical high (Liu and Chan 2013), an anomalous westward SST gradient in the WNP (Choi et al. 2015), as well as phase transitions of the PDO, Interdecadal Pacific Oscillation (IPO) (He et al. 2015; Hong et al. 2016; Hu et al. 2018; Zhao et al. 2018b), and the Atlantic Multidecadal Oscillation (AMO) (Zhang et al. 2018a). However, no consensus has been reached on the leading cause. Analysis from a longer period is also less covered in previous studies. Hence, the underlying mechanisms of WNP TC decadal variability remain open to debate and deserve further research.

It has been documented that ENSO SST indices not only exhibit interannual variability, but also display enhanced variance at lower frequencies (on decadal timescales) (An and Wang 2000; An and Jin 2000; Rodgers et al. 2004; Ren et al. 2013). This decadal component of ENSO is possibly a red noise process related to subtropical stochastic excitation of the Pacific meridional mode (Di Lorenzo et al. 2015) and/or the nonlinear rectification of interannual ENSO variability (Rodgers et al. 2004) possibly due to nonlinear zonal advection (Timmermann 2003; Hayashi and Jin 2017). As both ENSO and WNP TC activity exhibit variability on decadal timescales, the scientific question regarding their potential physical connection naturally arises. For example, the tropical Pacific experienced the longest-on-record El Niño-like state during the period of 1990–1995 (Trenberth and Hoar 1996), coinciding with extremely active TCs in the WNP. This implies that some kind of connection possibly exists between low-frequency WNP TC activity and the decadal state of the ENSO system. To our knowledge, this issue has not been elucidated in the aforementioned studies. Here we investigate the possible contribution of ENSO-associated decadal changes to the observed WNP TC activity shift during the mid-to-late 1990s based on both observations and coupled model simulations. We first identify a strong seasonal and spatial inhomogeneity in the decadal change of WNP TC activity, and then underline the role

of ENSO-associated decadal variability in driving vertical wind shear variability. In turn, this vertical wind shear variability modulates TC activity in certain sub-regions of the WNP on decadal timescales. In the reminder of this paper, Sect. 2 describes the data and method utilized in this study. The seasonal and spatial inhomogeneity of the TC decadal decrease is illustrated in Sect. 3. In Sect. 4 we explore the possible influences of ENSO-associated decadal variability based on both observational records and pre-industrial control (pi-control) simulations from the Coupled Model Intercomparison Project Phase 5 (CMIP5). The main conclusions and related discussions are summarized in Sect. 5.

2 Data and methodology

2.1 Datasets

The TC best-track data during 1951–2017 over the WNP are derived from the Japan Meteorological Agency (JMA; RSMC 2012), including the date, position, minimum surface pressure, and maximum surface wind speed (MSW). It should be noted that MSW is only available since 1977. Qualitatively consistent results (not displayed) can be drawn using best-track data from the Joint Typhoon Warning Center (JTWC) and the Shanghai Typhoon Institute of the China Meteorology Administration (Ying et al. 2014).

Several atmospheric and oceanic variables for the same period (1951–2017) were used to explore the decadal changes of large-scale environmental conditions. They are monthly global wind and relative humidity from the National Center for the Environmental Prediction/National Center for Atmospheric Research (Kalnay et al. 1996), as well as monthly global SST data derived from the National Oceanic and Atmospheric Administration (NOAA) Extended Reconstructed SST analysis, version 3 (Smith et al. 2008). Due to the relatively short observational period, we also examine preindustrial control (pi-control) simulations from 30 CMIP5 models (details for each model are listed in Table 1). The pi-control experiments simulate natural unforced climate variability without the influence from global warming by specifying constant orbital parameters, spectral solar irradiance, greenhouse gas concentrations, and natural aerosol forcing all at the year 1850 values (Taylor et al. 2012). The last 100 years of each simulation are analyzed and model variables are interpolated onto a common grid $2° \times 2°$ (same horizontal resolution with reanalysis datasets) using bilinear interpolation.

2.2 Methodology

The WNP in this study denotes the domain from $0°$ to $40°N$ and $100°E$ to $180°$. As MSW data is not available

Table 1 Detailed information about the CMIP5 models used in this paper (see http://www.ipcc-data.org/sim/gcm_monthly/AR5/Reference-Archive.html for more details about modeling center)

Number	Model name	Atmosphere (ocean) variable resolution (nlat × nlon)	Simulation length
1	ACCESS1-0	144×192 (300×360)	500
2	bcc-csm-1-1	64×128 (232×360)	500
3	bcc-csm-1-1-m	160×320 (232×360)	400
4	CanESM2	64×128 (192×256)	996
5	CCSM4	192×288 (384×320)	1051
6	CESM1-BGC	192×288 (384×320)	500
7	CESM1-CAM5	192×288 (384×320)	319
8	CESM1-FASTCHEM	192×288 (384×320)	222
9	CESM1-WACCM	96×144 (384×320)	200
10	CMCC-CESM	48×96 (149×182)	277
11	CMCC-CMS	96×192 (149×182)	500
12	CNRM-CM5	128×256 (292×362)	850
13	CNRM-CM5-2	128×256 (292×362)	359
14	FIO-ESM	64×128 (384×320)	800
15	GFDL-CM3	90×144 (200×360)	500
16	GFDL-ESM2G	90×144 (210×360)	500
17	GFDL-ESM2 M	90×144 (200×360)	500
18	GISS-E2-H-CC	89×144 (90×144)	251
19	GISS-E2-R	89×144 (90×144)	1200
20	HadGEM2-CC	144×192 (216×360)	241
21	HadGEM2-ES	144×192 (216×360)	577
22	IPSL-CM5A-LR	96×96 (149×182)	1000
23	IPSL-CM5A-MR	143×144 (149×182)	300
24	IPSL-CM5B-LR	96×96 (149×182)	300
25	MIROC5	128×256 (224×256)	700
26	MPI-ESM-LR	96×192 (220×256)	1000
27	MPI-ESM-MR	96×192 (404×802)	1000
28	MPI-ESM-P	96×192 (220×256)	1156
29	NorESM1-M	96×144 (384×320)	501
30	NorESM1-ME	96×144 (384×320)	252

before 1977, the TC genesis before is roughly estimated according to its intensity category (i.e. tropical storm intensity or above). After 1977, a TC is defined when its corresponding maximum surface wind speed averaged every minute (MSW_1) is not below 34 knots/s or the wind speed averaged every 10 min (MSW_{10}) is not below 30 knots/s ($MSW_{10} \approx 0.88 MSW_1$). This conversion had been adopted by the International Best Track Archive for Climate Stewardship (IBTrACS) project and various operational centers (Knapp et al. 2010). It should be pointed out that the difference between TC numbers derived using MSW and category is small and therefore do not significantly affect our conclusions. The genesis location is defined as the first position when a TC meets the threshold intensity. By counting the number of genesis locations and track positions every

6 h during each TC's lifetime in $5° \times 5°$ grid boxes, one can obtain the genesis density and track density of the TCs, respectively.

ENSO amplitude is measured by area-averaged SST anomalies in the Niño3.4 region (5°S–5°N, 120°W–170°W), and the ENSO events identification criterion is refered to the Climate Prediction Center (CPC) (3 month running mean of SST anomalies in Niño3.4 region meet a threshold of ± 0.5 °C and last for at least 5 consecutive overlapping seasons), which is also used in the operational monitoring system of China (Ren et al. 2018). The PDO and AMO indices are, respectively, represented by the leading principal component of SST anomalies over the North Pacific region (20°–70°N, 110°E–110°W) (Mantua et al. 1997) and the SST anomalies averaged over the North Atlantic region (0°–60°N, 0°–80°W) (Trenberth and Shea 2006). The instantaneous global-mean sea surface temperature has been removed from the SST anomalies to account for the nonlinear global warming trend as has been done in previous studies (Mantua et al. 1997; Trenberth and Shea 2006). For the observations, the PDO index is obtained directly from the University of Washington Joint Institute for the Study of the Atmosphere and Ocean (JISAO) (http://research.jisao.washington.edu/pdo/PDO.latest.txt). The tripole index for the IPO is based on the difference between the SST anomalies averaged over the central equatorial Pacific (10°S–10°N, 170°E–90°W) and the average of the SST anomalies in the Northwest (25°–45°N, 140°E–145°W) and Southwest (15°–50°S, 150°E–160°W) Pacific (Henley et al. 2015).

The zonal vertical wind shear (UVWS) is defined as the zonal wind difference between 200 and 850 hPa, which is almost the same metric as vertical wind shear due to the minor contribution from meridional wind shear (less than 5% in our study). Decadal variation of all indices and variables are computed using a 21-point Lanczos low-pass filter with a 10-year cutoff period. Statistical significance tests on atmospheric and oceanic variables were performed based on the two-tailed Student's t test. Considering that the number of yearly TCs follows a Poisson distribution instead of a Gaussian distribution (Chu and Zhao 2004; Chu et al. 2010; Tippett et al. 2011), we used a non-parametric bootstrap method to test the statistical significance of genesis and track density differences between different periods. This method has been extensively used in climate research as it can be applied to small sample sizes and makes no prior assumption about the statistical distribution (Chu and Wang 1997; Camargo and Sobel 2010). The adjusted effective sample size is calculated based on the following equation, and is adopted when testing the statistical significance of linear correlations (Pyper and Peterman 1998; Li et al. 2013a):

$$\frac{1}{N^{\text{eff}}} \approx \frac{1}{N} + \frac{2}{N} \sum_{j=1}^{N} \frac{N-j}{N} \rho_{xx}(j)\rho_{yy}(j),$$

where N and N^{eff} are sample size and equivalent effective sample size, respectively, and $\rho_{xx}(j)$ and $\rho_{yy}(j)$ represent the auto-correlations of sample X and Y at a lag time j, respectively.

3 Seasonal and spatial inhomogeneity of the TC decadal decrease

Figure 1 shows the time evolution of the annual-mean TC genesis number in the WNP from 1979 to 2017. Despite pronounced interannual variability, a distinct decadal decrease can be detected around 1994/1995, which is evidenced by an 11-year moving t test (not shown). The average TC genesis number is reduced from 27.9 for 1979–1994 to 23 for 1995–2012 (their difference amounts to roughly 20% of the climatological value). This TC genesis decadal change is similar to what previous studies found (Hsu et al. 2014; He et al. 2015; Hong et al. 2016; Zhang et al. 2018a). To better understand this decadal shift, we separate the whole period into three epochs: 1979–1994 (epoch1), 1995–2012 (epoch2), and 2013–2017 (epoch3). Note that the ending year of epoch2 is 2012 as TC genesis number is above the mean value thereafter and the tropical Pacific mean state shifted towards an El Niño-like state since then (Cha et al. 2018). In this section, the comparison between epoch1 and epoch2 is analyzed to focus on the decadal shift around the mid-1990s (the TC activity over the other epochs is examined later).

Due to the large spatial extent of the WNP region, we further divide the WNP into 5 subdomains, namely, the South China Sea (SCS), the southwest (SW), the southeast (SE), the northeast (NE), and the northwest (NW) (Fig. 2) according to previous studies (Wang and Chan 2002; Chen and Tam 2010). The monthly differences of TC genesis numbers in each subdomain between the two epochs are displayed
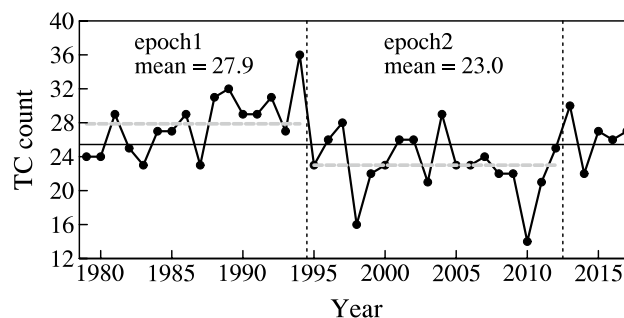

Fig. 1 Time evolution of annual TC genesis number in the WNP during 1979–2017. The vertical dashed lines separate the whole period into three subperiods (i.e., 1979–1994, 1995–2012, and 2013–2017) while horizontal black solid and grey dashed lines indicate the mean value for the annual TC genesis number during the whole period and the former two epochs, respectively
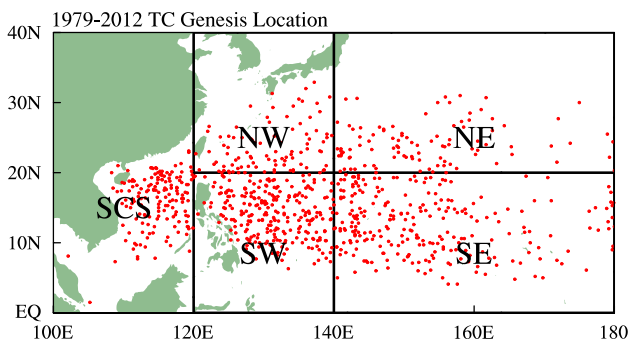
Fig. 2 Map of the WNP subdomains and TC genesis locations (red dots) for the whole period. SCS, SW, SE, NE, and NW represent the South China Sea, the southwest, southeast, northeast, and northwest sub-regions of the WNP, respectively

in Fig. 3. It is shown that the WNP TC decadal change exhibits a remarkable seasonality with a strong decrease mainly during the second half of the year (July–December) and relatively small changes during the first half of the year (January–June) (Fig. 3f). Among the five subdomains, the SE region (SE–WNP) displays the most pronounced decadal decrease during the second half of the year (Fig. 3b), resembling the pattern for the whole WNP (Fig. 3f) in terms of both seasonality and decreasing magnitude. The SE–WNP alone accounts for about 88% of the WNP TC decadal change, calculated by the contribution of the TC change in the SE-WNP to that in the whole WNP region. In contrast, this decadal change is absent in all other four subdomains (the contribution of each of the other regions is always less than 9%; Fig. 3).

To further validate the main contribution of the SE–WNP to the total WNP TC change, we show the spatial distribution
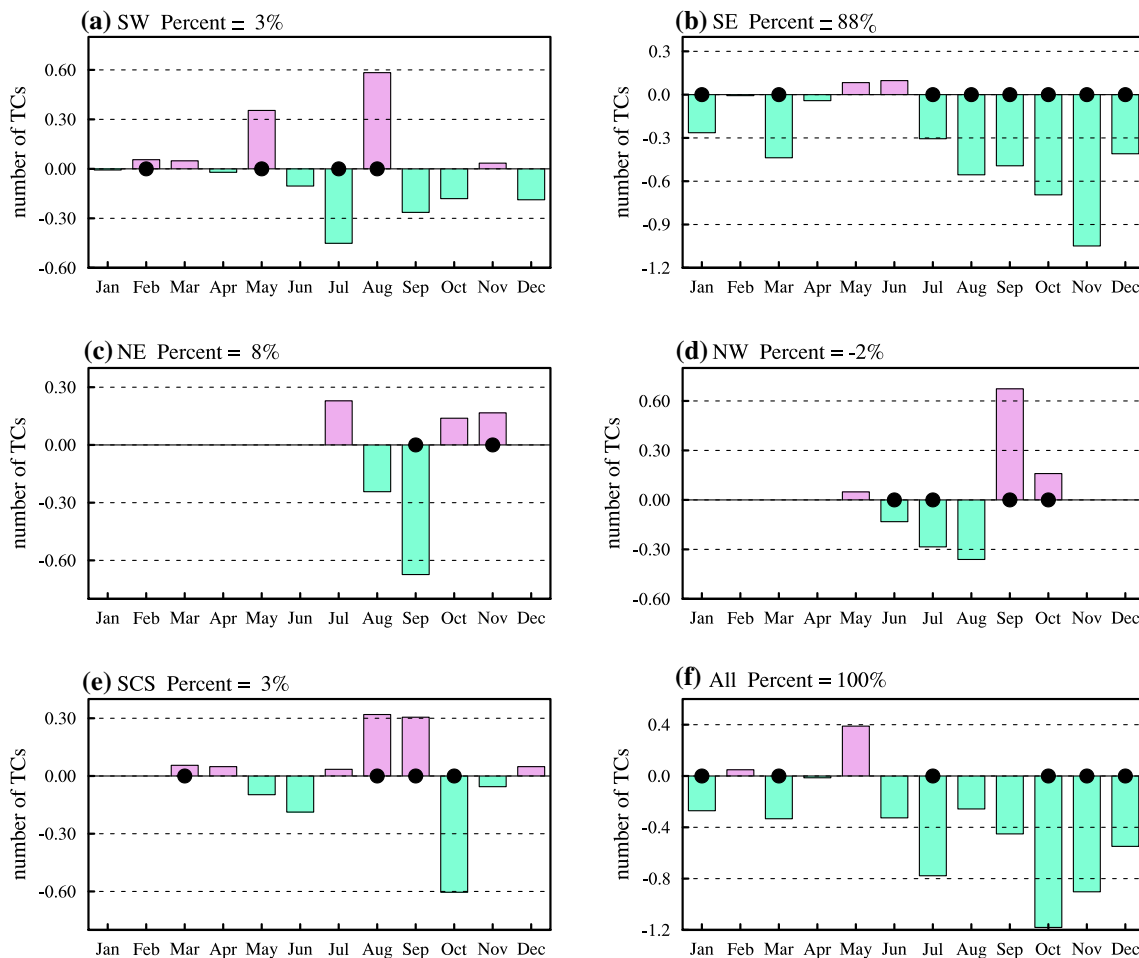
Epoch2-Epoch1

Fig. 3 The monthly differences of TC genesis number in regions **a** SW, **b** SE, **c** NE, **d** NW, **e** SCS, and **f** whole part of the WNP between epoch2 (1995–2012) and epoch1 (1979–1994). The percentage in each plot is calculated as the total monthly changes in each sub-region versus the changes in the whole WNP. The black dots indicate differences that are statistically significant above the 95% confidence level

of TC activity and atmospheric circulation differences between the two epochs (Fig. 4). Here, only the second half of the year (i.e., July–December) is considered since the robust decadal shift of the WNP TC occurs mainly during this part of the year. In contrast to epoch1, epoch2 is characterized by reduced genesis densities as well as prominent enhancement of the UVWS in the SE-WNP. The decrease is generally uniform in sign but not in magnitude. The severest decrease is located between 140°E and 160°E, which coincides with the overlapping region of UVWS enhancement and the dominant region of TC genesis climatology (Fig. 5). In contrast, TC tracks show a much clearer and more distinguishable decadal change pattern (Fig. 4b). Westward moving and northeastward recurving TC tracks display large reduction while northwestward recurving tracks show a slight increase. There is a characteristic anticyclonic circulation anomaly evident near 140°E and 15°N at 500 hPa, which might contribute to the TC track pattern change by inducing unfavorable steering flow for TCs moving westward or recurving to the northeast. The reduction of TC formation in the SE–WNP is also contributes to the TC track change.

It has long been recognized that the large-scale atmospheric circulation plays a critical role for TC genesis (e.g., Emanuel 2002; Murakami and Wang 2010). We next examine the contribution of several crucial WNP environmental conditions (i.e., UVWS, low-level vorticity, and middle-level humidity) that strongly affect TC genesis (e.g., Emanuel 2002; Camargo et al. 2007a; Murakami and Wang 2010; Li et al. 2013b) in Fig. 5. The decadal enhancement of UVWS

east of 140°E (i.e., the SE–WNP) is clearly seen in Fig. 5a during the second half of the year. It largely overlaps with the dominant region of TC genesis climatology, indicating its prominent impact. A strong UVWS tends to inhibit TC formation by tilting the vertical structure of storms and thereby disrupting organized deep convection (De Maria 1996). Therefore, the decadal change of UVWS corresponds well to the shift of the TC genesis in terms of both regionality and seasonality. We also show the difference of the zonal wind profile averaged over SE-WNP during the second half of the year between these two epochs (Fig. 5b). Compared with epoch1, both an easterly anomaly at lower levels and a westerly anomaly at upper levels contribute to the enhancement of UVWS in epoch2, with the change of upper level winds being approximately twice as large as the change of the lower level winds. In contrast, no clear decadal change of UVWS can be found in other seasons and other regions (Fig. 5a), a result that is consistent with the observed changes in TC activity. Other environmental factors affecting TC activity including relative vorticity at 850 hPa and relative humidity at 600 hPa are also shown (Fig. 5b, c). The statistically significant low-level vorticity decadal change mismatches climatology of TC activity for most of the season and areas except during October, November, and December (late season) in the SE–WNP, which is consistent with previous findings (Hsu et al. 2014). As a result, it plays a minor role in the decadal TC genesis decrease. Interestingly, middle-level moisture significantly increases along the 140°E and largely coincides with the climatology of TC genesis. The TC formation, however, does not show
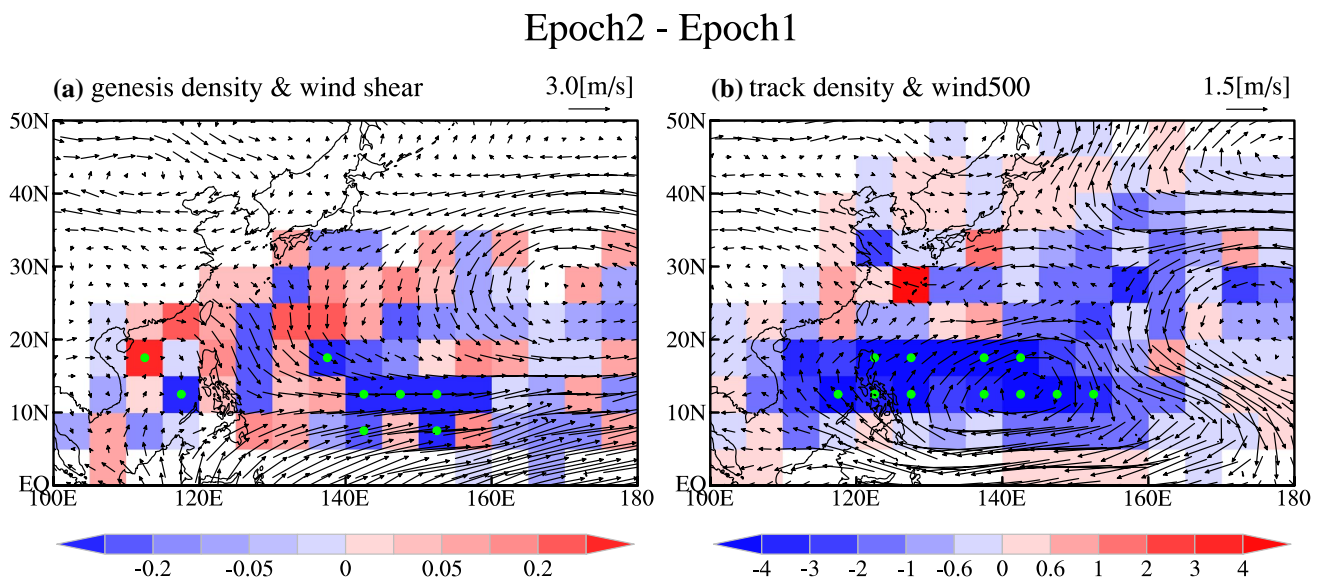
Epoch2 - Epoch1

Fig. 4 Differences of the **a** TC genesis densities (colors in number per year) and vertical wind shear (vectors in m/s), **b** track densities (colors in number per year) and 500 hPa wind (vectors in m/s) between the two epochs (1979–1994 and 1995–2012). Green dots in **a**, **b** represent TC genesis/track density differences that are statistically significant above the 95% confidence level

Fig. 5 Differences of **a** zonal vertical wind shear (shading), **b** zonal wind profile averaged in the SE region during the second half of the year, **c** vorticity at 850 hPa (shading), and **d** relative humidity at 600 hPa (shading) between the two epochs (1979–1994 and 1995–2012). TC genesis climatology (grey lines) are overlayed as reference. Meridional averages are calculated from the equator to 20°N for the Hovmöller diagrams. Stippled areas in **a**, **c** and **d**, and closed circles in **b**, indicate the differences that are statistically significant above the 90% confidence level. Units are shown at the top right of each plot
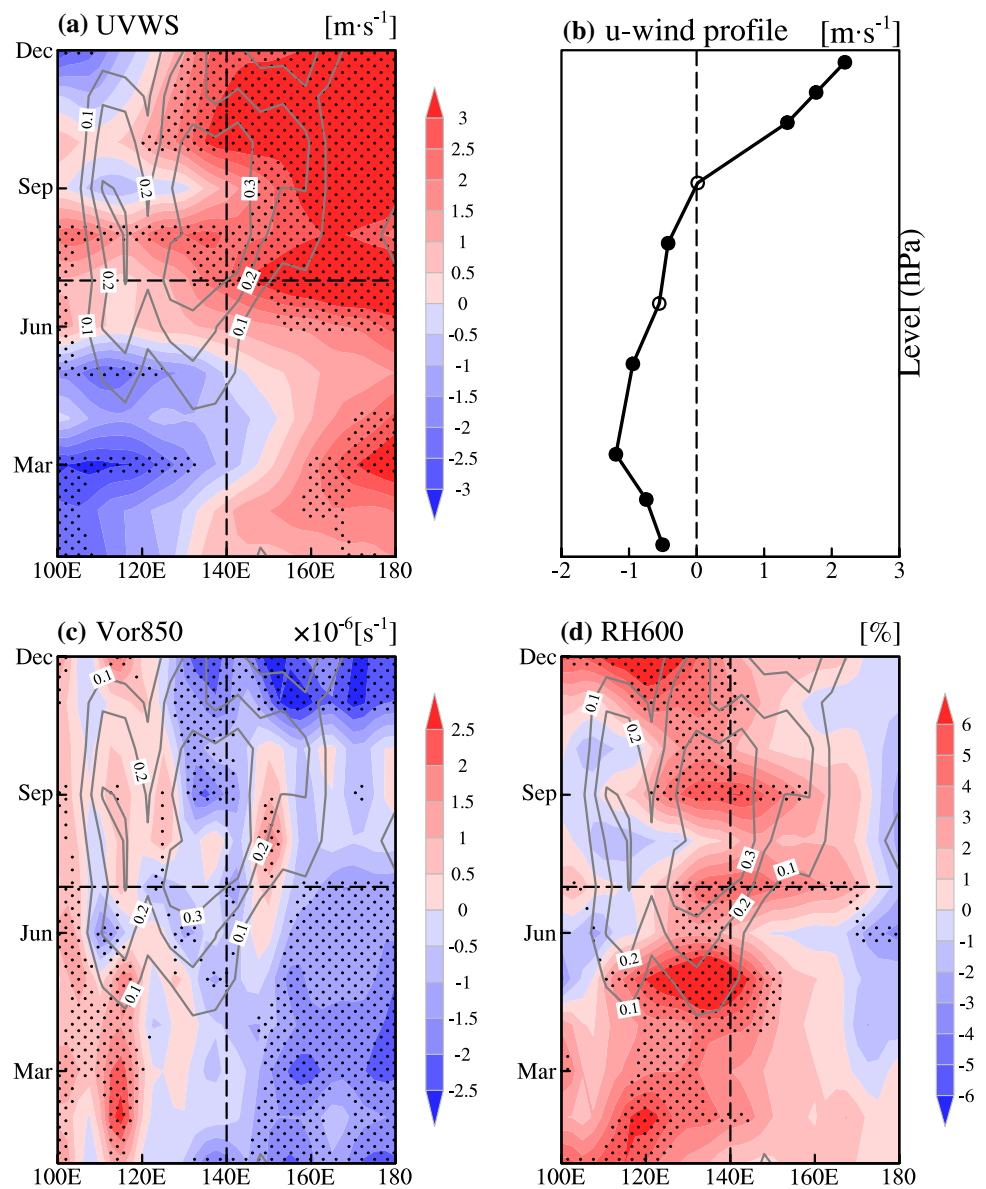
corresponding decadal changes, implying less essential role of thermodynamical fields for deep tropic TC activity on decadal timescale. In a word, the decadal enhancement of UVWS in the SE–WNP is the primary reason for the decadal TC genesis decrease since 1995.

4 Possible physical mechanisms

The above analysis highlights the importance of decadal changes in UVWS on WNP TC activity that occurred during the mid-1990s. The next scientific question that needs to be addressed is what possible mechanisms explain this decadal enhancement of UVWS. Considering the seasonal and spatial features of the TC genesis decadal decrease, we here focus on the TC decadal shift during the second half of

the year over the SE-WNP. Hereafter, the TC genesis number denotes the sum in the SE–WNP from July to December if not explicitly stated otherwise.

Many previous studies showed seasonal-dependent TC activity in the WNP in response to ENSO on interannual timescales (e.g., Wang and Chan 2002; Camargo et al. 2007b; Wang et al. 2013). Here we show a scatterplot of the Niño3.4 index and TC genesis number over SE–WNP (Fig. 6a) to examine their relationship considering our different TC season definition (i.e., July–December). These two indices exhibit a positive simultaneous correlation (R = 0.67, exceeding the 99% confidence level). El Niño events are generally accompanied by more TCs in the SE–WNP, while La Niña events by less. As shown in Fig. 6b, c, the UVWS exhibits a statistically significant anti-correlation with both Niño3.4 (R = −0.74) and TC genesis number (R = −0.85),
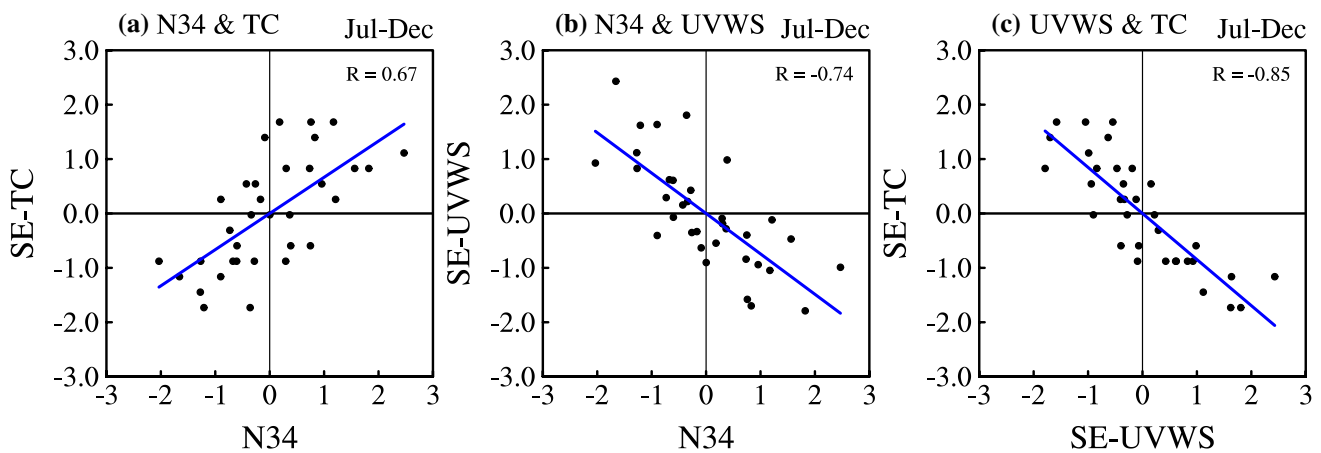
Fig. 6 Scatterplot of the **(a)** TC genesis number in the SE as a function of the Niño3.4 index, **(b)** UVWS index in the SE as a function of the Niño3.4 index, and **(c)** TC genesis number in the SE as a function of the UVWS index. All three indices are for the second half of the year and are normalized. The blue line in each plot represents the regression line using the linear least squares method

Table 2 El Niño and La Niña events identified for the 1979–2012 period

Period	El Niño	La Niña
1979–1994	1982, 1986, 1987, 1991, 1994	1984, 1988
1995–2012	1997, 2002, 2004, 2006, 2009	1995, 1998, 1999, 2000, 2007, 2010, 2011

in agreement with previous studies (e.g., Camargo et al. 2007b) arguing that the UVWS acts as a major mediation linking ENSO and WNP TC genesis numbers. Since TCs in the SE–WNP are closely related to ENSO variability on interannual timescales, we may wonder if this UVWS decadal change is associated with ENSO decadal variability. It is well known that the equatorial Pacific SSTs exhibit a significant cooling trend since 1979, resembling a La Niña-like pattern (e.g., Kosaka and Xie 2013, 2016; England et al. 2014; Trenberth 2015). Correspondingly, La Niña events occurred much more frequently during epoch2 (7 La Niña events) than during epoch1 (2 La Niña events) with El Niño events showing no obvious change in their occurrence frequency (Table 2). Since La Niña usually enhances UVWS in the SE–WNP and thus inhibits TC activity, more frequent La Niña events tend to be accompanied by a decreased TC genesis number. We show the difference of composited ENSO-related UVWS anomalies for these two epochs in Fig. 7. The differences in the SE–WNP region can largely explain the UVWS decadal change in terms of both regionality and seasonality.

However, it should be noted that phase transitions can also be detected for the two major SST interdecadal modes (i.e., PDO and AMO) during the mid-to-late 1990s, which might also contribute to the TC activity decadal change (Chan 2008; Hong et al. 2016; Zhang et al. 2018a). However, only one single cycle is insufficient to derive a robust relationship. To further examine the relationships between various modes of decadal climate variability and the TC genesis number, we show in Fig. 8 the decadal components of TC genesis number, UVWS index, Niño3.4 index, PDO, and AMO. The analysis period is extended to 1951–2017 here since it covers more phase transitions of the different modes of decadal variability. Here, the decadal component for all indices is derived using a 10-year low-pass filter. The 10-year low-pass filtered Niño3.4 index represents decadal variability of the equatorial Pacific SSTs. As shown in Fig. 8a, the TC genesis number, UVWS, and the Niño3.4 index exhibit consistent decadal swings if the sign of UVWS is reversed. The correlation coefficient between the low-frequency Niño3.4 index and the TC genesis number is 0.75, which is statistically significant above the 95% confidence level accounting for the effective degrees of freedom (df = 7). Interestingly, both the PDO and AMO experience a phase transition during the mid- to late-1990s, approximately matching the decadal shift of the TC genesis number; however, they fail to match the decadal variations of TC activity during earlier periods. The PDO and AMO have insignificant correlation coefficients with TC over the whole period (R = 0.43 for the PDO and R = −0.29 for the AMO). Therefore, it seems that the decadal variation of the tropical Pacific mean state could be the main driver of TC activity over the SE–WNP on decadal timescales, while robust effects of PDO and AMO on TC activity cannot be established. This can be further supported by the spatial relationship of UVWS within the larger Pacific domain with these three indices. The UVWS relationship with ENSO on decadal timescales is characterized by a meridional tripole pattern extending from the deep tropics to the extratropical North Pacific (Fig. 9a). The equatorial lobe of the correlation pattern is broadest and statistically most significant;

Fig. 7 Decadal change of **a** zonal vertical wind shear (shading), **b** zonal wind profile averaged in the SE-WNP region associated with ENSO years between epoch1 and epoch2. TC genesis climatology (grey lines) are overlayed as reference. Stippled areas in **a** and closed circles in **b** indicate the differences that are statistically significant above the 90% confidence level. Units are shown at the top right of each plot
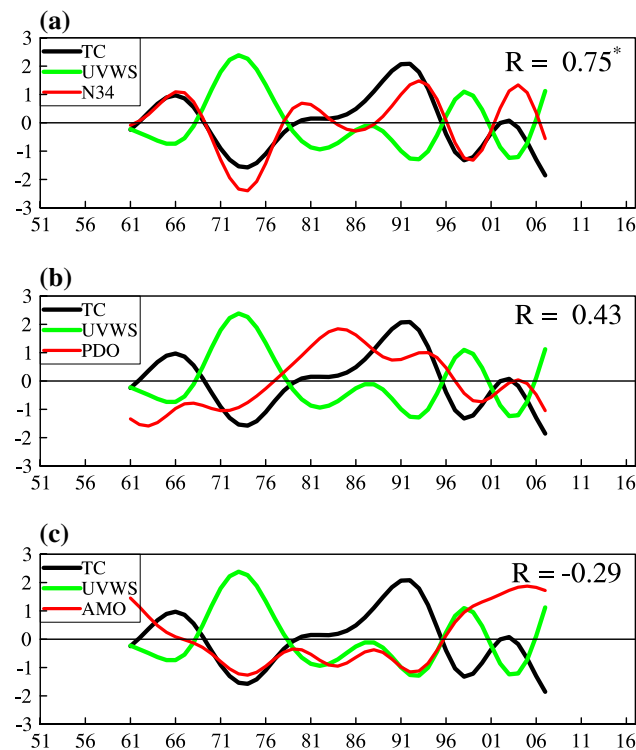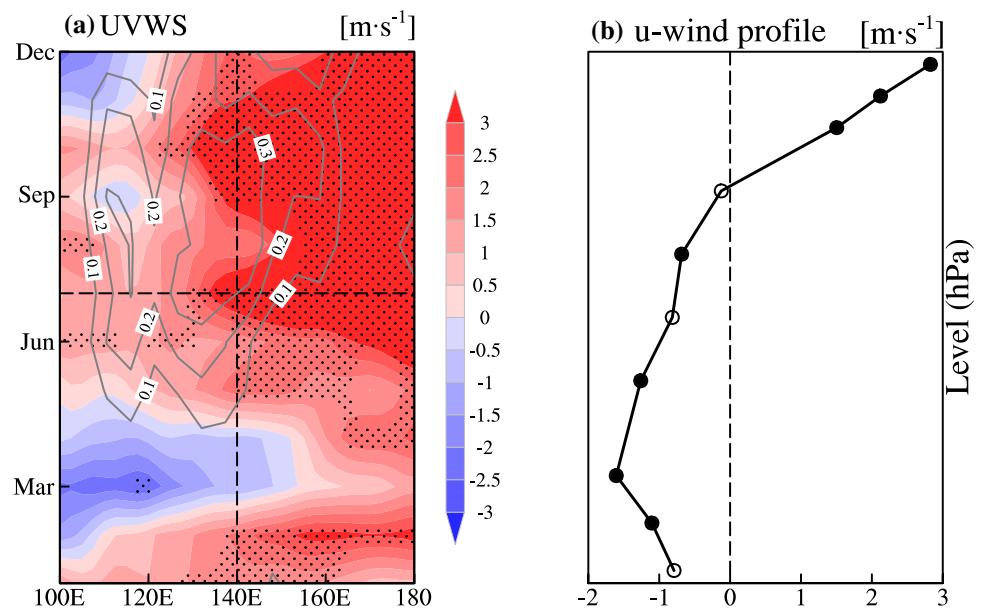

we can see that UVWS in the SE–WNP is tightly connected with ENSO on decadal timescales. No statistically significant correlations are detected for the UVWS with either the PDO or the AMO, although the correlation pattern with the PDO exhibits a similar spatial pattern to the correlations with the low-frequency ENSO component (Fig. 9b, c).

Next, we use the CMIP5 pi-control simulations to further examine possible linkages between TC activity and the Niño3.4, PDO, and AMO indices on decadal timescales, respectively. These simulations provide a much larger sample size to validate the conclusions drawn from the observations. Here, the UVWS is used to represent TC activity considering their close physical association and statistical relationship. The multi-model ensemble average of correlation patterns is displayed in Fig. 10. The simulations reproduce well the observed relationship between UVWS and the ENSO decadal signal (meridional tripole pattern) despite a slightly weaker and narrower meridional extent of the tropical lobe (Fig. 10a). Similar to the observations, the decadal modulation effects of the PDO and AMO on the UVWS explain little variance and lack inter-model consensus in the tropical Pacific. These model results support our hypothesis that the decadal swings of UVWS in the WNP region are mainly associated with the tropical Pacific decadal variability.

5 Conclusion and discussion

Our present study investigates the seasonal and spatial features of a decadal decrease in WNP TC activity around the mid-1990s and explores the possible contribution from equatorial Pacific SST decadal variability associated with
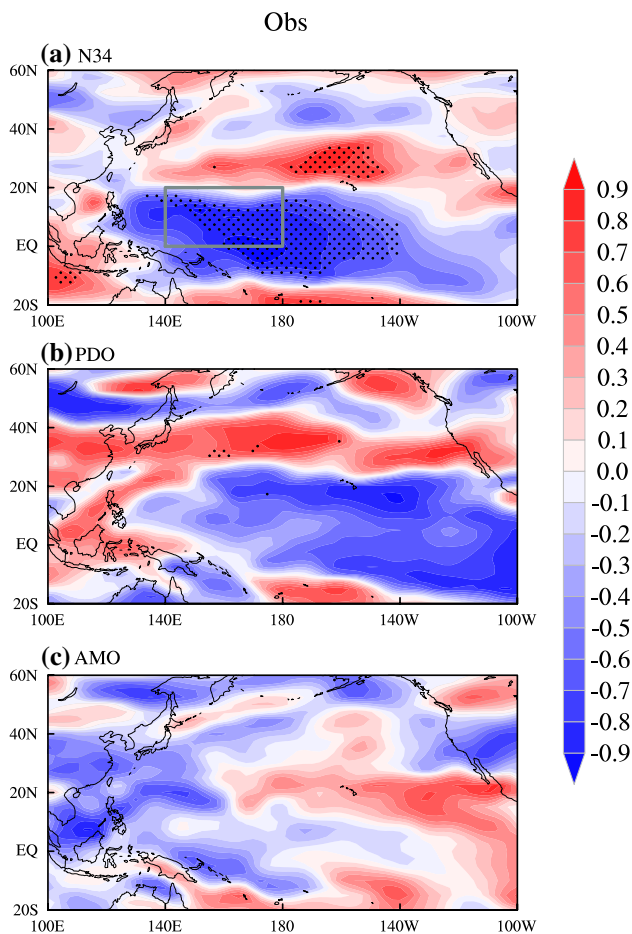

Fig. 8 Time evolutions of the TC genesis number (black line) and UVWS index (green line) together with **a** Niño3.4 index (red line), **b** PDO index (red line), and **c** AMO index (red line) on decadal timescales (21-point Lanczos low-pass filter with a 10-year cutoff period). Correlation coefficients between the TC genesis number and **a** Niño3.4, **b** PDO index, and **c** AMO index are shown on the top right of each plot with asterisk (*) indicating correlations that are statistically significant above the 95% confidence level

Fig. 9 Correlation coefficient of UVWS at each grid point with indices of **a** Niño3.4, **b** PDO, and **c** AMO on decadal timescales (same filter as used for Fig. 8). Stippled areas indicate values that are statistically significant above the 95% confidence level. The grey solid box denotes the SE–WNP

Fig. 10 Multi-model ensemble mean of UVWS correlation patterns with indices of **a** Niño3.4, **b** PDO, and **c** AMO on decadal timescales (same filter as used for Fig. 8) in CMIP5 pi-control simulations. Stippled areas indicate values that are statistically significant above the 95% confidence level

ENSO. We find that the decadal TC genesis decrease mainly occurs in the SE-WNP and during the second half of the calendar year, which is largely attributed to enhanced local UVWS. Correspondingly, much less TC tracks move to the western and northeastern parts of the region, while a slight increase of TC activity is found in the northwestern part of the WNP. Simultaneously, the equatorial Pacific exhibited a significant cooling trend, accompanied by more frequent occurrences of La Niña events during the 1995–2012 period compared with the preceding 1979–1994 period. More frequent La Niña events lead to a decreased TC genesis number in the SE–WNP after the mid-1990s, since La Niña tends to enhance the UVWS and thus inhibit TC activity. By extending the observational records (1951–2017) we can confirm that equatorial Pacific decadal variability associated with ENSO plays a critical role in the decadal swings of TC genesis. This statistical relationship between ENSO index and UVWS on decadal timescales can also be well
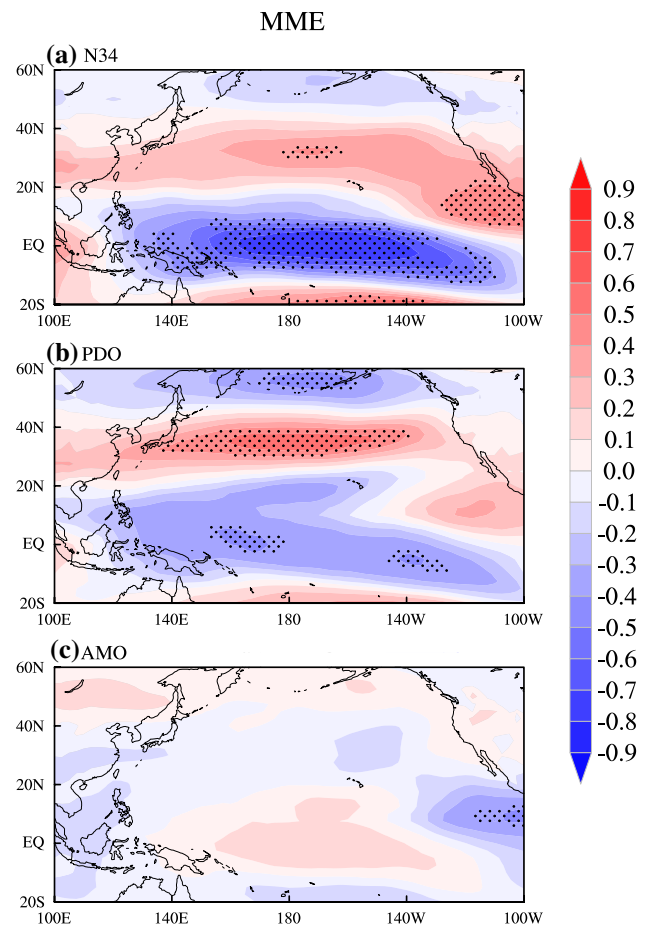
reproduced by CMIP5 pi-control simulations. In contrast, no robust relationship is found between TC-associated UVWS and the PDO and AMO, respectively, both in the extended observational data and in the coupled model simulations.

Here we emphasize the relationship between ENSO-associated decadal variability in the tropical Pacific and decadal variations of WNP TC activity. One might ask whether ENSO-associated decadal variability in the equatorial Pacific is partly driven by the PDO, since statistically significant connections can be found between ENSO and the PDO (Lin et al. 2018). Here we show the lead/lag cross correlation between the ENSO-associated decadal component and the PDO (Fig. 11) to elucidate their connection on decadal timescales. It is interesting that their correlation reaches a maximum when the low-frequency ENSO component leads the PDO by 1–3 years, both in the observations and models, which seems to be consistent with the hypothesis that ENSO forcing partly drives the PDO, even though
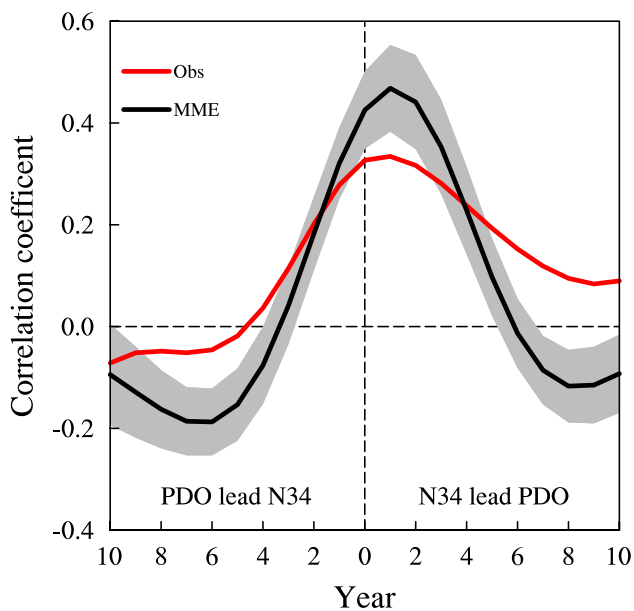
Fig. 11 Cross correlations between the Niño3.4 and PDO indices on decadal timescales (same filter as used for Fig. 8) for ERSSTv3b (red line) and the multi-model ensemble average (black line). The one standard deviation error estimate is indicated by grey shading for the models

activity variations; however, we cannot exclude the possibility that the AMO may play an indirect role for WNP TC activity by modulating ENSO variability. Our study suggests that tropical Pacific decadal variability in the equatorial Pacific is of great importance in regional climate decadal changes (for example, the WNP TC activity investigated in this study). Further research is needed to improve our understanding of the underlying mechanisms of ENSO-associated decadal variability in the equatorial Pacific and potentially utilize it for decadal predications of regional climate.

their physical connections remain a subject of active debate (e.g., Newman et al. 2016; Zhang et al. 2018b). Similarly, we also check the TC-IPO relationship on decadal timescales. The overall correlation coefficient ($R = 0.69$, $df = 6$) is higher than the TC-PDO correlation ($R = 0.4$, $df = 8$). However, by separating the IPO into tropical and extratropical parts based on the tripole index definition (Henley et al. 2015) to estimate their respective role on decadal TC variation, we again find that tropical low-frequency variability dominates ($R = 0.72$, $df = 6$) while the extratropical component plays a much lesser role ($R = 0.5$, $df = 6$). This supports our conclusion that the TC-IPO relationship is mainly determined by the tropical SST decadal variability.

Atlantic multidecadal variability is also argued to modulate the tropical Pacific mean state and ENSO activity (Timmermann et al. 2005; Dong et al. 2006; Chikamoto et al. 2015; Levine et al. 2017). For instance, a positive AMO could weaken ENSO variability via the "atmospheric bridge", which results in weakened trade winds, a deeper thermocline, and reduced vertical stratification in the equatorial Pacific Ocean (Dong et al. 2006). However, this relationship between the AMO and ENSO activity seems to disappear after the late 1990s (see Fig. 1b in Dong et al. 2006). This demonstrates that the decadal AMO modulation of ENSO activity is still not fully understood and deserves future attention. Here we focus on possible reasons for the decadal variation of WNP TC activity. We cannot find a statistically significant AMO signal in decadal WNP TC

References

An S-I, Jin F-F (2000) An eigen analysis of the interdecadal changes in the structure and frequency of ENSO mode. Geophys Res Lett 27:2573–2576. https://doi.org/10.1029/1999GL011090

An S-I, Wang B (2000) Interdecadal change of the structure of the ENSO mode and its impact on the ENSO frequency*. J Clim 13:2044–2055. https://doi.org/10.1175/1520-0442(2000)013%3c2044:ICOTSO%3e2.0.CO;2

Ashok K, Behera SK, Rao SA et al (2007) El Niño Modoki and its possible teleconnection. J Geophys Res. https://doi.org/10.1029/2006jc003798

Camargo SJ, Sobel AH (2005) Western North Pacific tropical cyclone intensity and ENSO. J Clim 18:2996–3006. https://doi.org/10.1175/JCLI3457.1

Camargo SJ, Sobel AH (2010) Revisiting the influence of the quasi-biennial oscillation on tropical cyclone activity. J Clim 23:5810–5825. https://doi.org/10.1175/2010JCLI3575.1

Camargo SJ, Emanuel KA, Sobel AH (2007a) Use of a genesis potential index to diagnose ENSO effects on tropical cyclone genesis. J Clim 20:4819–4834. https://doi.org/10.1175/JCLI4282.1

Camargo SJ, Robertson AW, Gaffney SJ et al (2007b) Cluster analysis of typhoon tracks. Part I: general properties. J Clim 20:3635–3653. https://doi.org/10.1175/JCLI4188.1

Camargo SJ, Sobel AH, Barnston AG, Klotzbach PJ (2010) The influence of natural climate variability on tropical cyclones, and seasonal forecasts of tropical cyclone activity. Global perspectives on tropical cyclones from science to mitigation. World Scientific, Singapore, pp 325–360

Cha S-C, Moon J-H, Song YT (2018) A recent shift toward an El Niño-Like ocean state in the tropical Pacific and the resumption of ocean warming. Geophys Res Lett 45:11,885–11,894. https://doi.org/10.1029/2018gl080651

Chan JC (2008) Decadal variations of intense typhoon occurrence in the western North Pacific. Proc R Soc A Math Phys Eng Sci 464:249–272. https://doi.org/10.1098/rspa.2007.0183

Chen G, Tam C-Y (2010) Different impacts of two kinds of Pacific Ocean warming on tropical cyclone frequency over the western North Pacific: IMPACTS OF OCEAN WARMING ON TC

FREQUENCY. Geophys Res Lett. https://doi.org/10.1029/2009gl041708

Chikamoto Y, Timmermann A, Luo J-J et al (2015) Skilful multi-year predictions of tropical trans-basin climate variability. Nat Commun. https://doi.org/10.1038/ncomms7869

Choi Y, Ha K-J, Ho C-H, Chung CE (2015) Interdecadal change in typhoon genesis condition over the western North Pacific. Clim Dyn 45:3243–3255. https://doi.org/10.1007/s00382-015-2536-y

Chu P-S, Wang J (1997) Tropical cyclone occurrences in the vicinity of Hawaii: are the differences between El Niño and non–El Niño years significant? J Clim 10:2683–2689

Chu P-S, Zhao X (2004) Bayesian change-point analysis of tropical cyclone activity: the central north pacific case*. J Clim 17:4893–4901. https://doi.org/10.1175/JCLI-3248.1

Chu P-S, Zhao X, Ho C-H et al (2010) Bayesian forecasting of seasonal typhoon activity: a track-pattern-oriented categorization approach. J Clim 23:6654–6668. https://doi.org/10.1175/2010JCLI3710.1

De Maria M (1996) The effect of vertical shear on tropical cyclone intensity change. J Atmos Sci 53:2076–2087

Di Lorenzo E, Liguori G, Schneider N et al (2015) ENSO and meridional modes: a null hypothesis for Pacific climate variability. Geophys Res Lett 42:9440–9448. https://doi.org/10.1002/2015GL066281

Dong B, Sutton RT, Scaife AA (2006) Multidecadal modulation of El Niño–Southern Oscillation (ENSO) variance by Atlantic Ocean sea surface temperatures. Geophys Res Lett. https://doi.org/10.1029/2006gl025766

Du Y, Yang L, Xie S-P (2011) Tropical Indian Ocean influence on northwest Pacific tropical cyclones in summer following strong El Niño*. J Clim 24:315–322. https://doi.org/10.1175/2010JCLI3890.1

Emanuel K (2002) A simple model of multiple climate regimes: CLIMATE REGIMES. J Geophys Res Atmos 107:ACL 4-1–ACL 4-10. https://doi.org/10.1029/2001jd001002

England MH, McGregor S, Spence P et al (2014) Recent intensification of wind-driven circulation in the Pacific and the ongoing warming hiatus. Nat Clim Change 4:222–227. https://doi.org/10.1038/nclimate2106

Ha Y, Zhong Z (2015) Decadal change in tropical cyclone activity over the South China Sea around 2002/03. J Clim 28:5935–5951. https://doi.org/10.1175/JCLI-D-14-00769.1

Ha Y, Zhong Z, Sun Y, Lu W (2014) Decadal change of South China Sea tropical cyclone activity in mid-1990s and its possible linkage with intraseasonal variability: decadal Change of SCS TC Activity. J Geophys Res Atmos 119:5331–5344. https://doi.org/10.1002/2013JD021286

Hayashi M, Jin F-F (2017) Subsurface nonlinear dynamical heating and ENSO asymmetry: subsurface NDH and ENSO asymmetry. Geophys Res Lett 44:12,427–12,435. https://doi.org/10.1002/2017gl075771

He H, Yang J, Gong D et al (2015) Decadal changes in tropical cyclone activity over the western North Pacific in the late 1990s. Clim Dyn 45:3317–3329

Henley BJ, Gergis J, Karoly DJ et al (2015) A tripole index for the interdecadal Pacific oscillation. Clim Dyn 45:3077–3090. https://doi.org/10.1007/s00382-015-2525-1

Hong C-C, Wu Y-K, Li T (2016) Influence of climate regime shift on the interdecadal change in tropical cyclone activity over the Pacific Basin during the middle to late 1990s. Clim Dyn 47:2587–2600. https://doi.org/10.1007/s00382-016-2986-x

Hsu P-C, Chu P-S, Murakami H, Zhao X (2014) An abrupt decrease in the late-season typhoon activity over the western North Pacific. J Clim 27:4296–4312. https://doi.org/10.1175/JCLI-D-13-00417.1

Hu F, Li T, Liu J et al (2018) Decrease of tropical cyclone genesis frequency in the western North Pacific since 1960s. Dyn Atmos Oceans 81:42–50. https://doi.org/10.1016/j.dynatmoce.2017.11.003

Huo L, Guo P, Hameed SN, Jin D (2015) The role of tropical Atlantic SST anomalies in modulating western North Pacific tropical cyclone genesis. Geophys Res Lett 42:2378–2384. https://doi.org/10.1002/2015GL063184

Kalnay E, Kanamitsu M, Kistler R et al (1996) The NCEP/NCAR 40-year reanalysis project. Bull Am Meteorol Soc 77:437–471. https://doi.org/10.1175/1520-0477(1996)077%3c0437:TNYRP%3e2.0.CO;2

Kao H-Y, Yu J-Y (2009) Contrasting Eastern-Pacific and Central-Pacific types of ENSO. J Clim 22:615–632. https://doi.org/10.1175/2008JCLI2309.1

Kim J-H, Ho C-H, Kim H-S et al (2008) Systematic variation of summertime tropical cyclone activity in the western North Pacific in relation to the Madden–Julian Oscillation. J Clim 21:1171–1191. https://doi.org/10.1175/2007JCLI1493.1

Kim H-M, Webster PJ, Curry JA (2011) Modulation of North Pacific tropical cyclone activity by three phases of ENSO. J Clim 24:1839–1849. https://doi.org/10.1175/2010JCLI3939.1

Knapp KR, Kruk MC, Levinson DH et al (2010) The international best track archive for climate stewardship (IBTrACS): unifying tropical cyclone data. Bull Am Meteorol Soc 91:363–376. https://doi.org/10.1175/2009BAMS2755.1

Knutson TR, McBride JL, Chan J et al (2010) Tropical cyclones and climate change. Nat Geosci 3:157–163. https://doi.org/10.1038/ngeo779

Kosaka Y, Xie S-P (2013) Recent global-warming hiatus tied to equatorial Pacific surface cooling. Nature 501:403–407. https://doi.org/10.1038/nature12534

Kosaka Y, Xie S-P (2016) The tropical Pacific as a key pacemaker of the variable rates of global warming. Nat Geosci 9:669–673. https://doi.org/10.1038/ngeo2770

Kug J-S, Jin F-F, An S-I (2009) Two types of El Niño events: cold tongue El Niño and warm pool El Niño. J Clim 22:1499–1515. https://doi.org/10.1175/2008JCLI2624.1

Levine AFZ, McPhaden MJ, Frierson DMW (2017) The impact of the AMO on multidecadal ENSO variability: aMO IMPACTS ON ENSO. Geophys Res Lett 44:3877–3886. https://doi.org/10.1002/2017GL072524

Li RCY, Zhou W (2013) Modulation of western North Pacific tropical cyclone activity by the ISO. Part I: genesis and intensity. J Clim 26:2904–2918. https://doi.org/10.1175/JCLI-D-12-00210.1

Li RCY, Zhou W (2014) Interdecadal change in South China sea tropical cyclone frequency in association with zonal sea surface temperature gradient. J Clim 27:5468–5480. https://doi.org/10.1175/JCLI-D-13-00744.1

Li J, Sun C, Jin F-F (2013a) NAO implicated as a predictor of Northern Hemisphere mean temperature multidecadal variability: NAO AS A PREDICTOR OF NHT VARIABILITY. Geophys Res Lett 40:5497–5502. https://doi.org/10.1002/2013GL057877

Li Z, Yu W, Li T et al (2013b) Bimodal character of cyclone climatology in the Bay of Bengal modulated by monsoon seasonal cycle. J Clim 26:1033–1046. https://doi.org/10.1175/JCLI-D-11-00627.1

Lin I-I, Chan JCL (2015) Recent decrease in typhoon destructive potential and global warming implications. Nat Commun. https://doi.org/10.1038/ncomms8182

Lin R, Zheng F, Dong X (2018) ENSO frequency asymmetry and the Pacific Decadal Oscillation in observations and 19 CMIP5 Models. Adv Atmos Sci 35:495–506. https://doi.org/10.1007/s00376-017-7133-z

Liu KS, Chan JCL (2013) Inactive period of western North Pacific tropical cyclone activity in 1998–2011. J Clim 26:2614–2630. https://doi.org/10.1175/JCLI-D-12-00053.1

Mantua NJ, Hare SR, Zhang Y et al (1997) A Pacific interdecadal climate oscillation with impacts on Salmon production. Bull

Am Meteorol Soc 78:1069–1079. https://doi.org/10.1175/1520-0477(1997)078%3c1069:APICOW%3e2.0.CO;2

Matsuura T, Yumoto M, Iizuka S (2003) A mechanism of interdecadal variability of tropical cyclone activity over the western North Pacific. Clim Dyn 21:105–117. https://doi.org/10.1007/s00382-003-0327-3

Mei W, Xie S-P (2016) Intensification of landfalling typhoons over the northwest Pacific since the late 1970s. Nat Geosci 9:753–757. https://doi.org/10.1038/ngeo2792

Murakami H, Wang B (2010) Future change of North Atlantic tropical cyclone tracks: projection by a 20-km-mesh global atmospheric model. J Clim 23:2699–2721. https://doi.org/10.1175/2010JCLI3338.1

Newman M, Alexander MA, Ault TR et al (2016) The Pacific decadal oscillation, revisited. J Clim 29:4399–4427. https://doi.org/10.1175/JCLI-D-15-0508.1

Peduzzi P, Chatenoux B, Dao H et al (2012) Global trends in tropical cyclone risk. Nat Clim Change 2:289–294. https://doi.org/10.1038/nclimate1410

Pyper BJ, Peterman RM (1998) Comparison of methods to account for autocorrelation in correlation analyses of fish data. Can J Fish Aquat Sci 55:2127–2140. https://doi.org/10.1139/cjfas-55-9-2127

Ren H-L, Jin F-F, Stuecker F, Xie MR (2013) ENSO regime change since the Late 1970s as manifested by two types of ENSO. J Meteorol Soc Jpn Ser II 91:835–842. https://doi.org/10.2151/jmsj.2013-608

Ren H-L, Lu B, Wan J et al (2018) Identification standard for ENSO events and its application to climate monitoring and prediction in China. J Meteorol Res 32:923–936. https://doi.org/10.1007/s13351-018-8078-6

Rodgers KB, Friederichs P, Latif M (2004) Tropical Pacific decadal variability and its relation to decadal modulations of ENSO. J Clim 17:3761–3774. https://doi.org/10.1175/1520-0442(2004)017%3c3761:TPDVAI%3e2.0.CO;2

RSMC (2012) Regional specialized meteorological Centers–Tokyo Typhoon Center tropical cyclone data. Available online at http://www.jma.go.jp/jma/jma-eng/jma-center/rsmc-hp-pub-eg/besttrack.html. Accessed 11 Dec 2018

Smith TM, Reynolds RW, Peterson TC, Lawrimore J (2008) Improvements to NOAA's historical merged Land–Ocean surface temperature analysis (1880–2006). J Clim 21:2283–2296. https://doi.org/10.1175/2007JCLI2100.1

Tao L, Wu L, Wang Y, Yang J (2012) Influence of tropical indian ocean warming and ENSO on tropical cyclone activity over the western North Pacific. J Meteorol Soc Jpn 90:127–144. https://doi.org/10.2151/jmsj.2012-107

Taylor KE, Stouffer RJ, Meehl GA (2012) An overview of CMIP5 and the experiment design. Bull Am Meteorol Soc 93:485–498. https://doi.org/10.1175/BAMS-D-11-00094.1

Timmermann A (2003) Decadal ENSO amplitude modulations: a nonlinear paradigm. Global Planet Change 37:135–156. https://doi.org/10.1016/S0921-8181(02)00194-7

Timmermann A, An S-I, Krebs U, Goosse H (2005) ENSO suppression due to weakening of the North Atlantic thermohaline circulation. J Clim 18:3122–3139. https://doi.org/10.1175/JCLI3495.1

Timmermann A, An S-I, Kug J-S et al (2018) El Niño–Southern Oscillation complexity. Nature 559:535–545. https://doi.org/10.1038/s41586-018-0252-6

Tippett MK, Camargo SJ, Sobel AH (2011) A poisson regression index for tropical cyclone genesis and the role of large-scale vorticity in genesis. J Clim 24:2335–2357. https://doi.org/10.1175/2010JCLI3811.1

Trenberth KE (2015) Has there been a hiatus? Science 349:691–692. https://doi.org/10.1126/science.aac9225

Trenberth KE, Caron JM (2000) The Southern Oscillation revisited: sea level pressures, surface temperatures, and precipitation. J Clim 13:4358–4365. https://doi.org/10.1175/1520-0442(2000)013%3c4358:TSORSL%3e2.0.CO;2

Trenberth KE, Hoar TJ (1996) The 1990–1995 El Niño–Southern Oscillation event: longest on record. Geophys Res Lett 23:57–60. https://doi.org/10.1029/95GL03602

Trenberth KE, Shea DJ (2006) Atlantic hurricanes and natural variability in 2005. Geophys Res Lett. https://doi.org/10.1029/2006gl026894

Vecchi GA, Soden BJ (2007) Effect of remote sea surface temperature change on tropical cyclone potential intensity. Nature 450:1066–1070. https://doi.org/10.1038/nature06423

Wallace JM, Rasmusson EM, Mitchell TP et al (1998) On the structure and evolution of ENSO-related climate variability in the tropical Pacific: lessons from TOGA. J Geophys Res Oceans 103:14241–14259. https://doi.org/10.1029/97JC02905

Wang B, Chan JC (2002) How strong ENSO events affect tropical storm activity over the western North Pacific. J Clim 15:1643–1658

Wang C, Li C, Mu M, Duan W (2013) Seasonal modulations of different impacts of two types of ENSO events on tropical cyclone activity in the western North Pacific. Clim Dyn 40:2887–2902. https://doi.org/10.1007/s00382-012-1434-9

Wang X, Wang C, Zhang L, Wang X (2015) Multidecadal variability of tropical cyclone rapid intensification in the western North Pacific. J Clim 28:3806–3820. https://doi.org/10.1175/JCLI-D-14-00400.1

Wang C, Wang B, Wu L (2018a) Abrupt breakdown of the predictability of early season typhoon frequency at the beginning of the twenty-first century. Clim Dyn. https://doi.org/10.1007/s00382-018-4350-9

Wang Q, Li J, Li Y et al (2018b) Modulation of tropical cyclogenesis location and frequency over the Indo-Western North Pacific by the intraseasonal Indo-Western Pacific convection oscillation during the boreal extended summer. J Clim 31:1435–1450. https://doi.org/10.1175/JCLI-D-17-0085.1

Ying M, Zhang W, Yu H et al (2014) An overview of the China meteorological administration tropical cyclone database. J Atmos Ocean Technol 31:287–301. https://doi.org/10.1175/JTECH-D-12-00119.1

Zhan R, Wang Y, Wu C-C (2011) Impact of SSTA in the East Indian Ocean on the frequency of northwest Pacific tropical cyclones: a regional atmospheric model study. J Clim 24:6227–6242. https://doi.org/10.1175/JCLI-D-10-05014.1

Zhan R, Wang Y, Ying M (2012) Seasonal forecasts of tropical cyclone activity over the western North Pacific: a review. Trop Cyclone Res Rev 1:18

Zhan R, Wang Y, Wen M (2013) The SST gradient between the southwestern Pacific and the Western Pacific warm pool: a new factor controlling the northwestern Pacific tropical cyclone genesis frequency. J Clim 26:2408–2415. https://doi.org/10.1175/JCLI-D-12-00798.1

Zhang W, Graf H-F, Leung Y, Herzog M (2012) Different El Niño types and tropical cyclone landfall in East Asia. J Clim 25:6510–6523. https://doi.org/10.1175/JCLI-D-11-00488.1

Zhang W, Li H, Jin F-F et al (2015) The annual-cycle modulation of meridional asymmetry in ENSO's atmospheric response and its dependence on ENSO zonal structure. J Clim 28:5795–5812. https://doi.org/10.1175/JCLI-D-14-00724.1

Zhang W, Vecchi GA, Murakami H et al (2016) The Pacific meridional mode and the occurrence of tropical cyclones in the western North Pacific. J Clim 29:381–398. https://doi.org/10.1175/JCLI-D-15-0282.1

Zhang W, Vecchi GA, Villarini G et al (2017a) Statistical-dynamical seasonal forecast of western North Pacific and East Asia landfalling tropical cyclones using the GFDL FLOR coupled

climate model. J Clim 30:2209–2232. https://doi.org/10.1175/JCLI-D-16-0487.1

Zhang W, Vecchi GA, Villarini G et al (2017b) Modulation of western North Pacific tropical cyclone activity by the Atlantic Meridional Mode. Clim Dyn 48:631–647. https://doi.org/10.1007/s00382-016-3099-2

Zhang W, Vecchi GA, Murakami H et al (2018a) Dominant role of Atlantic Multidecadal Oscillation in the recent decadal changes in western North Pacific tropical cyclone activity. Geophys Res Lett 45:354–362. https://doi.org/10.1002/2017GL076397

Zhang Y, Xie S-P, Kosaka Y, Yang J-C (2018b) Pacific decadal oscillation: tropical Pacific forcing versus internal variability. J Clim 31:8265–8279. https://doi.org/10.1175/JCLI-D-18-0164.1

Zhao J, Zhan R, Wang Y (2018a) Global warming hiatus contributed to the increased occurrence of intense tropical cyclones in the coastal regions along East Asia. Sci Rep. https://doi.org/10.1038/s41598-018-24402-2

Zhao J, Zhan R, Wang Y, Xu H (2018b) Contribution of Interdecadal Pacific Oscillation to the recent abrupt decrease in tropical cyclone genesis frequency over the western North Pacific since 1998. J Clim. https://doi.org/10.1175/jcli-d-18-0202.1

Zhao C, Ren H-L, Eade R et al (2019) MJO modulation and its predictability of boreal summer tropical cyclone genesis over northwest Pacific in Met Office Hadley Centre and Beijing climate center seasonal prediction systems. Quart J R Meteorol Soc. https://doi.org/10.1002/qj.3478

Publisher's Note Springer Nature remains neutral with regard to jurisdictional claims in published maps and institutional affiliations.